Numerical Simulation of Electrochemical Processes at a Tubular Electrode. Application to Spectroscopy

O.V. Klymenko[1], **J. Kulys**[2]

[1]Mathematical and Computer Modelling Laboratory
Kharkov National University of Radioelectronics
14 Lenin Avenue, Kharkov, 61166, Ukraine
klymenko@kture.kharkov.ua

[2]Department of Chemistry and Bioengineering
Vilnius Gediminas Technical University
Saulėtekio ave. 11, LT-10223 Vilnius, Lithuania

Abstract.   A model of spectroelectrochemical cell design based on a tubular working electrode with optical fibers connected to a spectrometer entering it from two ends is built. Both current and absorbance responses of the cell are numerically simulated and the operation regimes are determined in terms of ranges of governing parameters for chronoamperometry and linear sweep voltammetry.

Keywords: numerical simulation, tubular electrode, spectroelectrochemistry, absorbance.

1   Introduction

Spectroscopical methods coupled with usual electrochemical techniques allow additional advantages compared to purely electrochemical measurements through independently measured absorbance of the solution and/or its dependence on the wave length of the light shone through the system. There exist a variety of spectroelectrochemical methods designed to achieve particular goals and enhance the sensitivity of measurements [1].

In this paper we present a model of a tubular spectroelectrochemical cell (TSC) (Fig. 1) aimed at precise characterisation of the solution composition within a gold tube working electrode under various electrochemical conditions. The TSC consists of a tubular working electrode filled with a solution of an electroactive species A and with two optical fibers entering the tube from both ends and connected to a spectrometer in order to measure the overall absorbance of the solution filling the tube. The reference and counter electrodes are not shown in the scheme in Fig. 1 but it is assumed that their positioning allows for uniform accessibility of the tubular electrode walls to mass transport of species A and the product of the electrode reaction, B (i.e. the potential distribution along the working electrode may be assumed uniform).
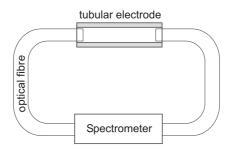
Fig. 1. Scheme of the spectroelectrochemical setup based on a tubular working electrode.

A number of studies have been published previously on hydrodynamic tubular electrodes [2–8]. The latter have many advantages for electroanalytical purposes but generally do not allow spectroscopic measurements to be performed *in situ* except electron spin resonance spectroscopy (ESR) [9] which is not within the scope of the proposed experimental setup. Therefore these works are mainly focused on purely electrochemical measurements.

Two essential advantages of the TSC setup can be mentioned. The amount of solution in the tubular reactor can be as small as 10^{-4} cm^3. At the same time the concentration of a component (depolarizer) can be low due to long (1 cm) optical path length. For this reason the tubular electrode configuration for the first time was used for the investigation of biological systems [10, 11].

The task of our investigation is to model the current response of the TSC and the corresponding absorbance distribution under potential step and linear sweep voltammetry conditions.

2   Mathematical model

Consider an electron transfer reaction

$$\text{A} - ne \rightleftarrows \text{B} \tag{1}$$

taking place at the inner surface of a tubular electrode of radius r_0 (see Fig. 1) under chronoamperometric or voltammetric conditions and characterized by the forward, k_f, and reverse, k_b, rate constants which are potential-dependent and follow the Butler-Volmer kinetics:

$$k_f = k_0 \exp\left(\frac{n(1-\alpha)F}{RT}\big(E - E^0\big)\right), \quad k_b = k_0 \exp\left(-\frac{n\alpha F}{RT}\big(E - E^0\big)\right), \tag{2}$$

where k_0 is the standard electrochemical rate constant, n the number of electrons transferred, α the transfer coefficient, E the applied potential, E^0 the standard potential of the redox couple A/B, F is the Faraday constant, R is the universal gas constant, and T is the temperature.

Diffusion mass transport of the species A inside the tubular electrode follows the second Fick's law formulated in the cylindrical coordinates:

$$\frac{\partial c}{\partial t} = D\left(\frac{\partial^2 c}{\partial r^2} + \frac{1}{r}\frac{\partial c}{\partial r}\right),$$

(3)

where $c = [A]$ is the concentration of species A, with uniform initial concentration in the solution bulk:

$$t = 0: \quad c(r,0) = c_0$$

(4)

and the following boundary conditions for $t > 0$:

$$r = 0: \quad \partial c/\partial r = 0;$$

(5a)

$$r = r_0: \quad -D\partial c/\partial r = k_f c - k_b(c_0 - c).$$

(5b)

In writing the latter boundary condition we have assumed that the diffusion coefficients of species A and B are equal so that at any time and any position in the space the sum of their concentrations remains constant, i.e. $[A] + [B] = c_0$.

The electric current flowing through the surface of the tubular electrode is given by the following expression

$$I(t) = -2\pi n F r_0 L D \frac{\partial c}{\partial r}\bigg|_{r=r_0},$$

(6)

where L is the length of the electrode. Note that the minus sign appears in (6) due to the multiplication of the flux, $j = -D\partial c/\partial r$, by the outer normal unit vector to the simulation domain, n, which in this case points "to the right", i.e. $n = 1$ (this is opposite to the majority of classical cases where the electrode is located "on the left" and then $n = -1$ giving a "plus" sign in the current expression for the anodic current).

The changes in the concentrations of species A and B are monitored using a spectrometer through two optical fibres inserted into the tubular electrode from both ends as described in the Introduction. Such a configuration allows registering variations of the average concentrations, i.e.

$$\psi(t) = \frac{2L}{r_0^2}\left(\varepsilon_A \int_0^{r_0} c(r,t)r\,\mathrm{d}r + \varepsilon_B \int_0^{r_0} \big(c_0 - c(r,t)\big)r\,\mathrm{d}r\right).$$

(7)

where $\psi(t)$ is the absorbance at time t, L is the optical length of the solution sample which is taken equal to the electrochemically active part of the tube, ε_A and ε_B are molar extinction coefficients (in $\mathrm{M}^{-1}\mathrm{cm}^{-1}$) of species A and B respectively.

Since absorbance is proportional to the sum of amounts of species A and B in the solution with the corresponding weighting coefficients ε_A and ε_B in the absence of homogeneous reactions involving either of species A and B, the same quantity may be

obtained by integrating the flux of species A (or, equally, that of B) to obtain the changes in the amounts of species A and B as:

$$\psi(t) = \varepsilon_A L c_0 - (\varepsilon_B - \varepsilon_A)\frac{1}{nF\pi r_0^2}\int\limits_0^t I(t)\,\mathrm{d}t$$

$$= L\left(\varepsilon_A c_0 - (\varepsilon_B - \varepsilon_A)\frac{2D}{r_0}\int\limits_0^t \left(\frac{\partial c}{\partial r}\right)_{r=r_0}\,\mathrm{d}t\right). \tag{8}$$

3 Dimensionless model

In order to define the main governing parameters of the system we introduce the following dimensionless parameters and variables

$$R = \frac{r}{r_0}; \quad \tau = \frac{Dt}{r_0^2}; \quad C = \frac{c}{c_0}; \quad K_0 = \frac{k_0 r_0}{D}; \quad \sigma = \frac{F r_0^2}{RTD}\nu, \tag{9}$$

where ν is the voltammetric scan rate (V/s).

The mathematical model in the dimensionless coordinates takes the form:

$$\frac{\partial C}{\partial \tau} = \frac{\partial^2 C}{\partial R^2} + \frac{1}{R}\frac{\partial C}{\partial R} \tag{10}$$

with the initial condition

$$\tau = 0: \quad C(R, 0) = 1 \tag{11}$$

and boundary conditions ($\tau > 0$):

$$R = 0: \quad \partial C/\partial R = 0; \tag{12a}$$
$$R = 1: \quad -\partial C/\partial R = K_f C - K_b(1 - C). \tag{12b}$$

The dimensionless overpotential, θ, variation under linear sweep voltammetry is defined by

$$\theta = \theta_{start} + \sigma\tau, \tag{13}$$

where $\theta_{start} = F(E_{start} - E^0)/(RT)$.

The dimensionless current (flux) is defined as

$$f = \frac{I}{2\pi nFLDc_0} = -\left.\frac{\partial C}{\partial R}\right|_{R=1}. \tag{14}$$

and the normalized change in the absorbance may be expressed as

$$
\begin{aligned}
\Psi(\tau) = \frac{\Psi}{\varepsilon_B L c_0} &= 1 + 2\left(\frac{\varepsilon_A}{\varepsilon_B} - 1\right) \int\limits_0^1 CR\,\mathrm{d}R \\
&= \frac{\varepsilon_A}{\varepsilon_B} + 2\left(\frac{\varepsilon_A}{\varepsilon_B} - 1\right) \int\limits_0^\tau \left(\frac{\partial C}{\partial R}\right)_{R=1} \mathrm{d}\tau,
\end{aligned}
\tag{15}
$$

where the two expressions at the right are equally valid and the absorbance of species B is assumed nonzero (i.e. the product of the electrochemical reaction (1) is more likely to absorb light than the initial species A).

4 Numerical simulation

The differential equation (10) was discretised using the fully implicit finite difference method with 2nd order implicit time stepping [12]. All calculations reported here were performed on a PC equipped with the Intel Pentium D processor at 2.8 GHz and 512 MB of RAM using a program written in-house in Borland Delphi 7.

5 Results and discussion

Owing to the dimensionless quantities introduced in Section 3 the two measurable characteristics of the tubular spectroelectrochemical cell (current and absorbance) depend exclusively on the dimensionless time and the ratio of extinction coefficients ε_A and ε_B for the case of chronoamperometry. For voltammetry, the main governing parameters are the normalized heterogeneous rate constant K_0 and scan rate σ while absorbance also depends on the ratio of extinction coefficients. In the following we shall not consider the effects of varying transfer coefficient α onto the dimensionless current and absorbance and hence a value of 0.5 is assumed throughout the rest of this paper. Thus in the following we will consider the two cases of chronoamperometry and voltammetry and characterize the system responses as functions of governing parameters.

5.1 Chronoamperometry

An important feature of the tubular electrode is that it contains a finite volume of solution and therefore is subject to quick exhaustive electrolysis when all of species A is converted into B. This is exemplified in Fig. 2(a) which illustrates that, after an initial spike, the current quickly tends to zero. Thus it is important to determine the time window accessible to the tubular cell. By using the definition of the diffusion layer thickness for a planar electrode under Cottrellian conditions [1], $\delta \approx \sqrt{Dt}$, one can devise an upper estimate for the exhaustion time to be $t_{max} = r_0^2/D$. However, this value is too high since it does not take into account converging cylindrical diffusion. In fact, Cottrellian

behaviour in this system is observed only at extremely short times when the thickness of the diffusion layer is negligible compared to the tube radius, i.e. when $\tau = Dt/r_0^2 \ll 1$. Numerical simulation of chronoamperometry shows that already for dimensionless times $\tau \geq \tau_{planar} = 10^{-3}$ the deviation of the simulated current from the Cottrell equation exceeds 2 % (see Fig. 2(b)). From the same simulation one can deduce that after a dimensionless time $\tau = 0.61$ the amount of electroactive species A left in the solution drops to less than 2 % of the initial quantity, which results in strong current diminishment and therefore this value may be taken as the exhaustion time: $\tau_{exhaust} = 0.61$.
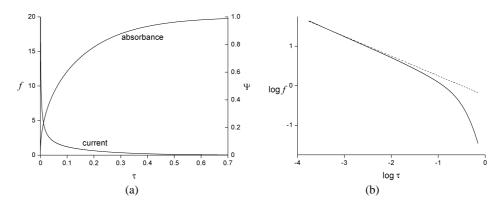

Fig. 2. Transient current at a tubular electrode (solid curve) compared to Cottrell current (dashed line).

It may be inferred from equation (15) that the dimensionless absorption Ψ changes between $\varepsilon_A/\varepsilon_B$ at $\tau = 0$ before the application of potential to the working electrode and 1 when the solution is completely exhausted. Therefore, if the absorbance of species A is not negligible compared to that of species B, the variation of the absorption during the experiment may be insufficient to be measurable by a spectrometer. Thus, when the condition

$$|1 - \varepsilon_A/\varepsilon_B| < 0.1 \qquad (16)$$

is not met the variation of the absorbance is too small for achieving good spectroscopic resolution. In the following the absorbance of A is assumed to be zero ($\varepsilon_A = 0$) so that dimensionless absorbance varies between 0 and 1 as depicted in Fig. 2(a). It is clear from the figure that in this case the absorbance Ψ at $\tau_{exhaust} = 0.61$ reaches 0.98 which corresponds to 98 % conversion of A into B.

5.2 Linear sweep voltammetry

In the case of linear sweep voltammetry the (dimensionless) scan rate σ defines the effective duration of electrolysis and therefore the following limiting cases may be identified: (i) planar diffusion limit when $\sigma > 10^4$, and (ii) thin layer cell limit when $\sigma < 1$.

The first limiting situation corresponds to short durations and therefore thin diffusion layers near the working electrode surface analogously to short-time behaviour under chronoamperometry. In this case voltammetric waves behave virtually as those at a planar electrode of the same surface area (see the plot in Fig. 3(a) for a reversible ET reaction, i.e. high K_0) with the same characteristic dependences of peak heights and potentials [1]. Since the total electrolysis duration in this case is very short the dimensionless absorbance Ψ cannot reach appreciable values although the current density at the electrode is high.

In the limiting situation (ii) the diffusion layer extends over the whole tube radius before the end of the voltammetric scan leading to exhaustive electrolysis and symmetrical bell-shaped current responses for reversible electron transfer (see Fig. 3(b)). In this case absorbance variation with potential is perfectly sigmoidal reaching the value of unity (full solution exhaustion) and centered at zero overpotential (Fig. 3(b)).
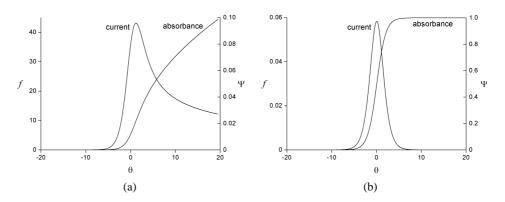

Fig. 3. Limiting cases in reversible linear sweep voltammetry ($K_0 = 10^4$): (a) planar diffusion limit ($\sigma = 10^4$); (b) thin layer cell limit ($\sigma = 0.5$).

For the general case of arbitrary dimensionless voltammetric scan rate σ and heterogeneous rate constant K_0 the peak current, f_p, and absorbance corresponding to the peak current, Ψ_p, are given in Fig. 4 (note the different directions of the $\log \sigma$ axis in Figs. 4(a) and 4(b)). It should be noted that for any values of K_0 both very slow and very fast voltammetric scan rates present no interest from the point of view of spectroscopy since in the former case variation in both the peak current and absorbance is negligible and in the latter case the values of absorbance are too low for quantitative measurements. Therefore the range of dimensionless scan rates suitable for both electrochemical and spectral measurements may be determined as

$$0.75 \leq \log \sigma \leq 2.75. \tag{17}$$

It is interesting to note that for low scan rates the limiting value of Ψ_p is 0.5 for a reversible ET reaction, but it is notably higher for the irreversible case as evident from Fig. 4(b). As was said above, slow linear sweep voltammetry in the reversible case leads to perfectly symmetrical sigmoidal absorbance distributions vs. overpotential with the

197

value 0.5 at $\theta = 0$ where the current has its peak. On the other hand, current response for irreversible ET for the same voltammetric scan rate is not symmetrical with a shallow rising part and a sharp drop after the peak, which is shifted to the right from $\theta = 0$. Thus it turns out that most of species A is converted into B before the current reaches its peak and the value of Ψ_p exceeds 0.5.
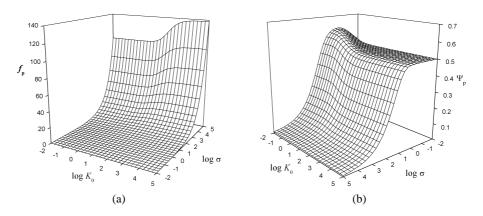
Fig. 4. Working surfaces for (a) the dimensionless peak current, f_p, and (b) absorbance at peak current, Ψ_p.

6   Conclusions

The presented design of a spectroelectrochemical cell with tubular working electrode and optical fibres inserted into it from the two ends allows simultaneous measurements of the electric current and absorbance of the solution to be performed. The numerical simulation of the diffusion pattern inside the tubular reactor for a simple electron transfer reaction has allowed the determination of limiting kinetic regimes and ranges of main parameters providing best conditions for both the electrochemical and spectral measurements. This cell design may find successful applications in the analysis of complex homogeneous chemical reactions coupled to the initial electron transfer at the working electrode surface. The modelling of the system involving both heterogeneous electron transfer and homogeneous reactions in the bulk solution is under consideration.

Acknowledgements

References

1. A. J. Bard, L. R. Faulkner, *Electrochemical Methods: Fundamentals and Applications*, 2nd edition, John Wiley & Sons, 2001.

2. L. N. Klatt, W. J. Blaedel, Quasi-reversible and irreversible tubular electrode, *Anal. Chem.*, **39**, pp. 1065–1072, 1967.

3. R. Alkire, A. A. Mirarefi, The current distribution within tubular electrodes under laminar flow, *J. Electrochem. Soc.*, **120**, pp. 1507–1515, 1973.

4. B. A. Coles, R. G. Compton, The theory of EC reactions at tubular electrodes, *J. Electroanal. Chem.*, **127**, pp. 37–42, 1981.

5. R. G. Compton, P. J. Daly, Current transients at a channel electrode produced by a potential step, *J. Electroanal. Chem.*, **178**, pp. 45–52, 1984.

6. J. Dutt, T. Singh, Linear sweep voltammetry at the tubular electrode, *J. Electroanal. Chem.*, **182**, pp. 259–266, 1985.

7. S. O. Engblom, D. K. Cope, D. E. Tallman, Diffusion current at the tubular band electrode by the integral equation method, *J. Electroanal. Chem.*, **406**, pp. 23–31, 1996.

8. M. Thompson, J. Davis, R. G. Compton, Theory of cyclic voltammetry in tubular electrodes under no flow conditions, *J. Electroanal. Chem.*, **587**, pp. 56–59, 2006.

9. A. J. Wain, M. Thompson, O.V. Klymenko, R. G. Compton, An improved configuration for simultaneous electrochemical ESR studies: a tubular electrode in a cylindrical cavity, *Phys. Chem. Chem. Phys.*, **6**, pp. 4018–4027, 2004.

10. T. Larsson, A. Lindgren, T. Ruzgas, Spectroelectrochemical study of cellobiose dehydrogenase and diaphorase in a thiol-modified gold capillary in the absence of mediators, *Bioelectrochem.*, **53**, pp. 243–249, 2001.

11. A. Christenson, E. Dock, L. Gorton, T. Ruzgas, Direct heterogeneous electron transfer of theophylline oxidase, *Biosen. Bioelectron.*, **20**, pp. 176–183, 2004.

12. R. D. Richtmyer, K. W. Morton, *Difference Methods for Initial-Value Problems*, 2nd edition, Wiley-Interscience, New York, 1967.